

---

**Biocybernetics and Biomedical Engineering**  
2006, Volume 26, Number 4, pp. 15-24

## **Texture Characterization for Hepatic Tumor Recognition in Multiphase CT**

**DOROTA DUDA<sup>1,2,\*\*</sup>, MAREK KRĘTOWSKI<sup>1</sup>,  
JOHANNE BÉZY-WENDLING<sup>2</sup>**

<sup>1</sup>*Faculty of Computer Science, Białystok Technical University, Białystok, Poland*

<sup>2</sup>*Laboratoire Traitement du Signal et de l'Image, INSERM, Université de Rennes1, Rennes, France*

A new approach to texture characterization from dynamic CT scans of the liver is presented. Images with the same slice position and corresponding to three typical acquisition phases are analyzed simultaneously. Thereby texture evolution during the propagation of contrast product is taken into account. The method is applied to recognizing hepatic primary tumors. Experiments with various sets of texture parameters and two classification methods show that simultaneous analysis of texture parameters derived from three subsequent acquisition moments improves the classification accuracy.

**Key words:** image processing, tissue characterization, texture analysis, liver CT images.

### **1. Introduction**

Computed Tomography (CT) is now a widely applied tool for diagnosis of hepatic tumors. The visual analysis of image series, acquired usually before a contrast product injection and during its propagation, enables doctors to detect lesions and to recognize, to a certain extent, the type of pathology. However, in most cases, visual inspection of CT scans could not be sufficient for proper image interpretation. Even for experienced radiologists, the correct differentiation of tumor affected tissue is a difficult task. The definitive diagnosis often requires invasive procedures like needle biopsy or even surgery, which carry a risk of complications. New computer-aided image processing methods (in particular methods of their texture analysis), in combination with effective classification algorithms, can considerably improve the accuracy of the diagnosis.

---

\* Correspondence to: Dorota Duda, Faculty of Computer Science, Białystok Technical University, ul. Wiejska 45A, 13-351 Białystok, Poland, e-mail: dordu@ii.pb.bialystok.pl

Extracting the information not normally detected by the human eye, those techniques could reduce or even eliminate the necessity of performing the invasive techniques [1].

An objective and explicit characterization of image regions is one of the crucial problems to deal with when a computer aided image analysis is performed. One of the most useful sources of information about analyzed image regions could be their texture [2]. The texture analysis consists in extracting a set of numerical parameters (so-called texture features) to characterize Regions of Interest (ROIs) defined in the organs under study. Each of the texture parameters expresses a specified property of the texture, like coarseness, homogeneity, or the local contrast. So far, a great variety of texture features extraction methods has been investigated. The proposed texture parameters are generally derived from simple (e. g. first order and gradient-based) statistics or more sophisticated (for example, based on co-occurrence matrices [3] or run-length matrices [4]) statistical properties of the image. Another possibility encompasses model-based approaches (e. g. fractals [5] and Markov fields [6]), transform methods (Fourier-based and Gabor-based [7], or wavelets [8]) or mathematical morphology operations [9]. The proposed methods of texture analysis, appropriately adapted for a particular clinical problem, have successfully been applied to a broad range of imaging modalities and diagnostic problems such as: classification of brain tumors (Magnetic Resonance Imaging) [10], solid breast nodules (ultrasound) [11], botulism on trabecular bone (X-ray radiograms) [12], coronary plaques (intravascular ultrasound) [13], or focal liver lesions, (Computed Tomography) [14]. An exhaustive review of the methods and their medical applications can be found in [1].

The first application of texture analysis for characterization of pathologically changed regions of liver tissue in tomographic images was presented in [15]. In the work it was shown that values of the gray level distribution derived from the run-length matrix were significantly different in normal and malignant tissue. Chen *et al.* [16] proposed an automatic diagnostic system for CT liver image classification that was able to automatically find, extract the liver boundary and to further classify its two major malignant lesions. The system used an artificial neural network in combination with fractal and co-occurrence features. A similar approach (the back-propagation neural network based on first order and co-occurrence features) was applied to recognizing a normal and abnormal liver [17]. In [18] the combination of four different fractal dimension estimators (corresponding to the power spectrum method, box counting method, the morphological fractal estimator and the kth-nearest neighbor method) and the fuzzy C-Means algorithm were applied to differentiate normal liver parenchyma from *hepatocellular carcinoma*. Recently, Gletsos *et al.* [14] presented a system that used co-occurrence descriptors and three sequentially placed feed-forward neural networks for classification of normal and pathological liver regions. Finally, in [19] a computer-aided diagnostic system to classify focal liver lesions by an ensemble of neural network and statistical classifiers was proposed. This system used first order statistics, co-occurrence matrix and gray-level difference matrix features, Laws' texture measures, and fractal dimension estimators to characterize four different types of

liver tissue. All aforementioned systems were applied to non-enhanced CT scans and did not consider dynamic CT.

In our investigations [20], texture classification of the hepatic metastasis was performed on the basis of dynamic CT. Images corresponding to three acquisition phases (non-enhanced images and after a contrast product injection, in arterial and portal phases) were analyzed separately. It was shown that considering the acquisition moments could improve the classification accuracy. In [21], for the first time, three CT scans with the same slice position and corresponding to three acquisition moments were analyzed simultaneously. The preliminary results showed that taking into account texture evolution when the contrast product is propagated led to a considerably better image recognition.

The remaining sections of the paper are organized as follows: in the next section the process of classifier induction based on image data is described and the method of construction of multi-phase feature vectors is presented. The third section contains the description, and results of the performed experiments in which two methods of classification (Dipolar Decision Trees and Support Vector Machines) were applied in recognition of two main primary hepatic tumors. The obtained results are discussed at the end of the section. Short conclusions and future plans follow in the last section.

## **2. Texture classification**

The first step in applying any computer-aided diagnostic tool based on the classifiers is preparation of the learning set, which will be used to generate the classifier. The learning set is created from the database of images for which the diagnosis is known. When the classifier is built it can be applied in prediction of new Regions of Interest.

### **2.1. Classifier induction based on the image database**

In figure 1, the schematic process of classifier induction based on previously gathered and described by the doctor-specialist image database is summarized. After the visual detection of pathological regions, ROIs are drawn inside the lesions. The localization of the concerned Regions of Interest can be performed manually or semi-automatically with the employment of adequate segmentation procedures. The tissue characterization of each ROI is then performed. It consists in calculation of the sets of texture parameters that will create feature vectors (each corresponding to an individual region) of a learning set. For each image region, the equivalent vector also includes the label (class) corresponding to the verified diagnosis. Sometimes the feature selection is then performed in order to choose the most relevant features, eliminate the redundant ones, reduce the dimensionality of feature vectors and limit the further computation time. Different approaches for feature selection towards multiphase liver CT images are investigated in [22]. Finally, the classifier is induced from the learning set composed of the labeled feature vectors. After its generation, the classifier can be used in recognition of unknown image regions. Figure 2 presents schematic process of classifier application

to the recognition of ROI. For a given image, a Region of Interest is traced but now the class of the concerned ROI is not known. The same set of features as it was utilized during the process of classifier induction is then calculated for this image region. Applying a set of previously generated classifiers allows us to make a decision and associate one of the classes with the analyzed ROI.

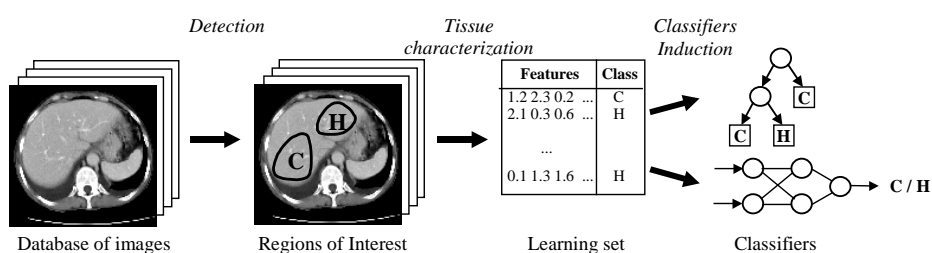


**Fig. 1.** Induction of the classifiers from the preprocessed database of images [20]. C and H stand for exemplary liver tissue classes: cirrhosis and hepatocellular carcinoma, respectively

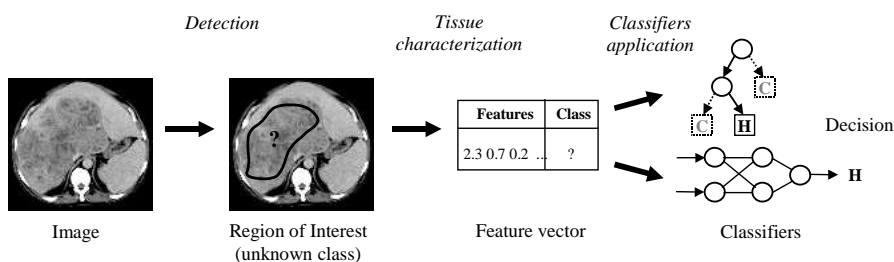


**Fig. 2.** Application of the classifiers to the recognition of unknown Region of Interest. C and H stand for exemplary liver tissue classes: cirrhosis and hepatocellular carcinoma, respectively

## 2.2. Texture evolution during propagation of contrast material

In clinical practice, when medical imaging is performed, diagnosis often bases on simultaneous analysis of image groups, in which each image presents in a different way the same part of the analyzed organ. Consecutive image series can be acquired with different acquisition parameters (e. g. repetition time and echo time for MRI) or different phases of contrast material propagation (for example – in CT of abdominal organs). When liver disorders are concerned, three scan series are usually acquired: the first – before the injection of the contrast product, the following two series are realized on contrast-enhanced images, in arterial and portal phases of contrast propagation. Radiologists commonly exploit an evolution of the tissue region appearance in the three

consecutive images (corresponding to the three aforementioned acquisition phases) as a discrimination factor in the hepatic tumor diagnosis.

When designing a computer-aided system for diagnosis of hepatic tumors, an analogous idea was adapted. Not only texture characteristics of the considered region are analyzed, but also their changes in the three acquisition moments. Figure 3 presents the scheme of construction of “multiphase” feature vectors. Three images in the picture present the same liver slice in the three acquisition moments (N – no contrast, A – arterial phase, P – portal phase). The same region of interest (with the same position and size) is then traced on the three images. Next, three groups of texture features are calculated (each feature vector corresponds to one of the three regions of interest). Finally, three vectors are concatenated in one “multiphase” vector, containing the parameters corresponding to the three acquisition moments.

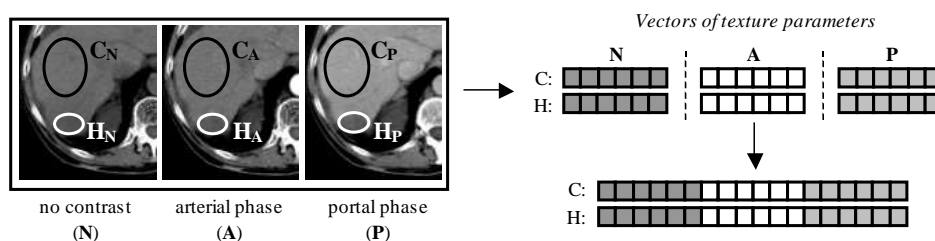


**Fig. 3.** Construction of the “multiphase” feature vectors describing the evolution of liver tissue appearance in the three consecutive images, corresponding to three acquisition phases: *N* (no contrast), *A* (arterial phase), *P* (portal phase). In each image, two Regions of Interest were traced:  $C_x$  for cirrhotic liver and  $H_x$  for liver affected by *hepatocellular carcinoma*, where index  $x$  corresponds to one of the three aforementioned acquisition phases

### 3. Experiments

The proposed approach to a multiphase texture characterization was applied in the classification of liver tumors in dynamic Computed Tomography. Three classes of ROIs were being recognized: the normal liver and its two main primary malignant lesions: *hepatocellular carcinoma* and *cholangiocarcinoma*.

#### 3.1 Experimental setup

A database of 495 images (165 images for each acquisition phase) from 22 patients was gathered in Eugene Marquis Center, the University Hospital in Rennes, France. The acquisitions were performed with a GE HiSpeed CT device and the standardized acquisition protocol was applied: helical scanning, with slice thickness 7 mm. For each patient, an appropriate amount of the contrast material was chosen (about 100 ml), and the injection was performed at 4 ml/s. The acquisition of the images in the arterial phase

started about 20 seconds after the contrast product injection. Images corresponding to the portal phase were acquired with delay of 50-60 s. All images had a size of 512x512 pixels with 8-bit gray levels and were represented in DICOM format.

For each tissue type and each acquisition phase 150 non-overlapped circular regions of interest of radii of 30-70 pixels were chosen. They were manually placed avoiding the biggest vessels. In questionable cases, when the radiological report did not a precise enough lesion location, the expert was asked to position the ROI. All the cases were confirmed by a histopathological analysis. Figure 4 presents examples of analyzed regions of interest corresponding to the analyzed classes of tissue in the three acquisition phases.

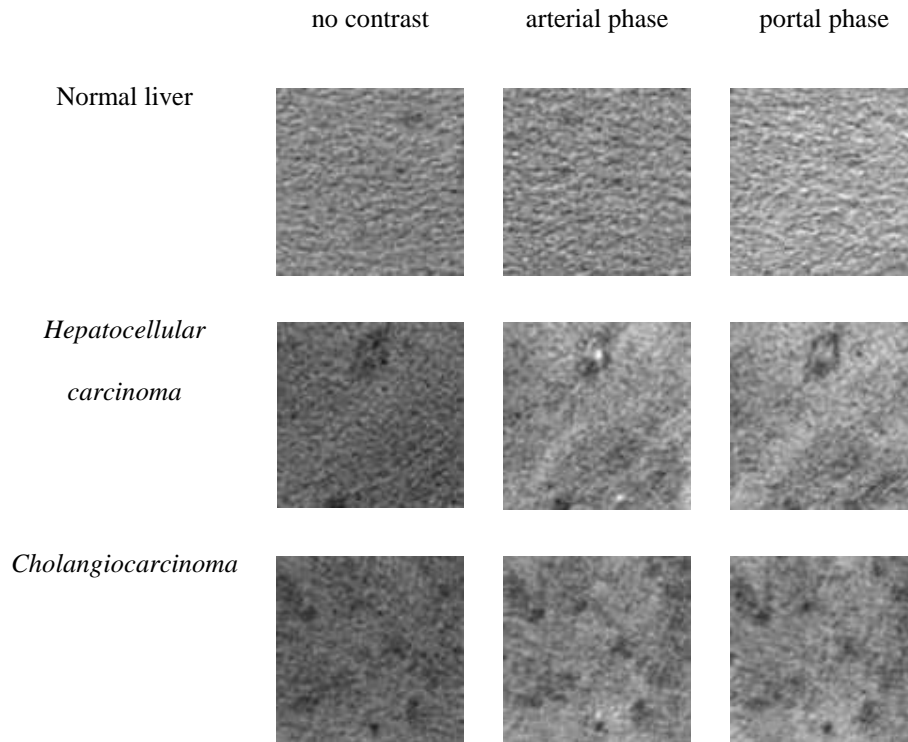


**Fig. 4.** Examples of analyzed textures extracted from hepatic CT images

### 3.2 Texture characterization and classification methods

In the presented experiments the following groups of texture features were extracted:

- 4 first order parameters (calculated from the gray level histogram) (*FO*),

- 
- entropy of image after filtering it with 14 pairs of zero-sum 5x5 Laws' filters (*Laws*),
  - 8 Run-Length Matrix features (*RLM*),
  - 11 Co-occurrence parameters (*COM*),
  - 35 parameters obtained with all of the aforementioned methods.

Co-occurrence Matrices and Run-Length Matrices were created for 4 standard directions of pixel pairs (pixel runs):  $0^\circ$ ,  $45^\circ$ ,  $90^\circ$ , and  $135^\circ$ . For these two methods, the number of gray levels was reduced from initially used 256 to 64. When creating Co-occurrence Matrices 5 pixel distances were taken into account (1, 2, 3, 4 and 5). Features obtained for different directions and different distances were averaged. For image filtration, 24 Laws' filters were considered. The sum of elements of every convolution matrix was equal to zero. Pairs of filtered images corresponding to the applied masks and their rotations were added. Images corresponding to symmetric masks were multiplied by two.

Four experiments were performed for each of aforementioned sets of features. In the first three ones, feature vectors corresponding to three acquisition phases (N, A, P) were analyzed separately. In the last one, "multiphase" feature vectors (created for three regions of interest corresponding to the three images in subsequent acquisition moments) were analyzed simultaneously. In each case, two classification methods were used for texture recognition: Dipolar Decision Trees (DDT) [23] and Support Vector Machines (SVM) [24]. The learning sets used for classifier induction were composed of 75 observations corresponding to each acquisition phase (225 observations in total). Test sets of equal number of feature vectors were used for classifier validation. For Dipolar Decision Trees, the weights of mixed dipoles were 1, 10, 100, 500 and 1000, while the weights of pure dipoles were equal to one. For Support Vector Machines, two kernel functions were used: polynomials with a degree ranging from 1 to 6, and Radial Basis Functions with parameter gamma ranging from  $10^{-6}$  to  $10^{-1}$ . For each of the cases, the best classification result was chosen. Tables 1 and 2 present the accuracy obtained for DDT and SVM classification methods, respectively.

### 3.3 Discussion

As it can be seen in Tables 1 and 2, the classification quality was generally high. For each classifier, the best results were obtained for groups of all texture features (in all cases the classification accuracy was greater than 90% for Support Vector Machines and was about 99% for Dipolar Decision Trees). For each case, a higher accuracy was observed for Dipolar Decision Trees (the highest differences in the classification accuracy could be noticed for RLM set of features, even more than 40% in the arterial phase). Finally, it can be observed that regardless of the texture analysis method and regardless of the classification method, the classification quality is significantly increased, when the feature vectors are composed of parameters from three subsequent acquisition moments (N + A + P). The highest classification accuracy (99.53%) was obtained for the group of all 35 texture features with Dipolar Decision Tree.

**Table 1.** Classification accuracy (%) obtained with DDT for different groups of texture features

|              | no contrast (N) | arterial phase (A) | portal phase (P) | N + A + P    |
|--------------|-----------------|--------------------|------------------|--------------|
| FO           | 90.16 ± 1.31    | 85.82 ± 1.48       | 90.40 ± 1.69     | 98.76 ± 0.73 |
| Laws         | 91.13 ± 0.84    | 92.27 ± 1.25       | 88.33 ± 2.20     | 95.11 ± 1.19 |
| COM          | 96.36 ± 0.88    | 94.29 ± 1.79       | 94.87 ± 0.83     | 99.67 ± 0.37 |
| RLM          | 95.53 ± 1.02    | 93.89 ± 1.28       | 95.45 ± 1.59     | 99.73 ± 0.42 |
| all features | 99.11 ± 0.74    | 98.89 ± 0.44       | 99.18 ± 0.62     | 99.53 ± 0.86 |

**Table 2.** Classification accuracy (%) obtained with SVM for different groups of texture features

|              | no contrast (N) | arterial phase (A) | portal phase (P) | N + A + P    |
|--------------|-----------------|--------------------|------------------|--------------|
| FO           | 82.46 ± 0.59    | 71.11 ± 0.69       | 74.44 ± 0.90     | 89.42 ± 0.91 |
| Laws         | 79.38 ± 1.24    | 71.42 ± 1.59       | 66.27 ± 1.08     | 82.44 ± 1.20 |
| COM          | 86.80 ± 0.63    | 78.71 ± 0.31       | 76.27 ± 0.66     | 91.47 ± 0.55 |
| RLM          | 71.02 ± 0.89    | 51.42 ± 0.66       | 56.50 ± 1.14     | 71.82 ± 1.87 |
| all features | 91.02 ± 0.86    | 90.09 ± 0.56       | 90.00 ± 0.83     | 95.87 ± 0.93 |

#### 4. Conclusions

In the work a new method of characterization of the texture from multiphase CT images was presented. Images with the same slice location and corresponding to three typical acquisition moments were analyzed simultaneously. In this way the texture evolution during the propagation of the contrast product was taken into account. The method was applied to recognizing normal liver and its two main primary tumors. Experiments with various sets of texture parameters and two classification methods showed that a simultaneous analysis of texture parameters derived from three subsequent acquisition moments considerably improved the classification accuracy.

In the future, the work on recognition of the tumor affected liver tissue based on multiphase CT will be continued. The methods of extracting other “multiphase” parameters will be investigated. An enlargement of the image database and introduction into it of new types of hepatic tissue (other types of tumors) is also planned. Finally, an analogous idea of texture characterization will be adapted for description of cerebral tumors (*gliomas*) in Magnetic Resonance Imaging. In this case an evolution of the texture parameters during propagation of the contrast material and their relation to changes of the acquisition parameters will be studied. This work has already begun in collaboration with the University Hospital in Caen (France).

#### Acknowledgement

The authors thank Dr. A Carsin and Dr. Y. Rolland for their clinical contribution to this study. This work was supported by the grant W/WI/1/05 from Białystok Technical University

---

## References

1. Bruno A., Collorec R., Bézy-Wendling J., Reuzé P., Rolland Y.: Texture analysis in medical imaging, In: Roux C., Coatrieux J. L. (Eds.): Contemporary Perspectives in Three-dimensional Biomedical Imaging, IOS Press, 1997, 133-164.
2. Haralick R. M.: Statistical and structural approaches to texture, Proc. IEEE, 1979, 67, 786-804.
3. Haralick R. M., Shanmugam K., Dinstein I.: Textural features for image classification. IEEE Transactions on Systems, Man and Cybernetics, 1973, 3:610-621.
4. Galloway M. M.: Texture analysis using gray level run lengths. Computer Graphics and Image Processing, 1975, 4:172-179.
5. Chen C., Daponte J. S., Fox M. D.: Fractal feature analysis and classification in medical imaging, IEEE Transactions on Medical Imaging, 1989, 8, 133-142.
6. Cross G. R., Jain A. K.: Markov random fields texture models. IEEE Transactions on Pattern Analysis and Machine Intelligence, 1985, 5(1):25-39.
7. Clausi D. A., Jernigan M. E.: Designing gabor filters for optimal texture separability. Pattern Recognition, 2000, 33:1836-1849.
8. Mallat S. G.: A theory for multiresolution signal decomposition: The wavelet representation. IEEE Transactions on Pattern Analysis and Machine Intelligence, 1989, 11(7):674-693.
9. Haralick R., Sternberg S. R., Zhuang X.: Image analysis using mathematical morphology. IEEE Transactions on Pattern Analysis and Machine Intelligence, 1989, 9(4):532-550.
10. Herlidou-Meme S., Constans J. M., Carsin B., Olivie D., Eliat P. A., Nadal-Desbarats L., Gondry C., Le Rumeur E., Idy-Peretti I., de Certaines J.D.: MRI texture analysis on texture test objects, normal brain and intracranial tumors. Magnetic Resonance Imaging, 2003, 21, 989-993.
11. Joo S., Yang Y. S., Moon W. K., Kim H. C.: Computer-aided diagnosis of solid breast nodules: use of an artificial neural network based on multiple sonographic features. IEEE Transactions on Medical Imaging, 2004, 23(10), 1292-1300.
12. Chappard D., Chennebault A., Moreau M., Legrand E., Audran, M., Basle M. F.: Texture analysis of X-ray radiograms is a more reliable descriptor of bone loss than mineral content in a rat model of localized disuse induced by the Clostridium botulinum toxin. Bone, 2001, 28(1), 72-79.
13. dos Santos Filho E., Yoshizawa M., Tanaka, A., Saijo, Y., Yambe T., Nitta, S.: Toward a neuro-fuzzy system for automatic segmentation and characterization of intravascular ultrasound images. SICE Annual Conference, 2003, Vol. 2, 1586-1589.
14. Gletsos M., Mougiakakou S. G., Matsopoulos G. K., Nikita K. S., Nikita A. S., Kelekis D.: A computer-aided diagnostic system to characterize CT focal liver lesions: design and optimization of a Neural Network classifier, IEEE Transactions on Information Technology in Biomedicine, 2003, 7(3), 153-162.
15. Mir A. H., Hanmandlu M., Tandon S. N.: Texture analysis of CT-images, IEEE Engineering in Medicine and Biology, 1995, 5, 781-786.
16. Chen E. L., Chung P. C., Chen C. L., Tsai H. M., Chang C. I.: An automatic diagnostic system for CT liver image classification. IEEE Transactions on Biomedical Engineering, 1998, 45(6), 783-794.

17. Husain S. A., Shigeru E.: Use of neural networks for feature based recognition of liver region on CT images, Proc. of the IEEE Signal Processing Society Workshop, 2000, Vol. 2, 831-840.
18. Sariyanni C. P. A., Asvestas P., Matsopoulos G. K., Nikita K. S., Nikita A. S. Kelekis D.: A fractal analysis of CT liver images for the discrimination of hepatic lesions: A comparative study, Proc. of the 23rd Annual EMBS International Conference, 2001, 1557-1560.
19. Valavanis I., Mougiakakou S. G., Nikita K. S., Nikita A.: Computer aided diagnosis of CT focal liver lesions by an ensemble of neural network and statistical classifiers, Proc. of the IEEE International Joint Conference on Neural Networks, 2004, Vol. 3, 1929-1934.
20. Krętowski M., Bezy-Wendling J., Duda D.: Classification of hepatic metastasis in enhanced CT images by dipolar decision tree, Proc. of 19th GRETSI, 2003, 327-330.
21. Duda D., Krętowski M., Bézy-Wendling J.: Texture-based classification of hepatic primary tumors in multiphase CT. Proc. of 7th MICCAI, LNCS Vol. 3217, Springer-Verlag, 2004, 1050-1051.
22. Duda D., Krętowski M., Bézy-Wendling J.: Texture analysis in medical image classification. Statistics and Clinical Practice, Lecture Notes of ICB Seminars, Vol. 70, 2005, 83-89.
23. Bobrowski L., Krętowski M.: Induction of multivariate decision trees by using dipolar criteria, LNCS Vol. 1910, Springer-Verlag, 2000, 331-336.
24. Vapnik V.: The Nature of Statistical Learning Theory, Springer-Verlag, New York, 1995.